Original Article

Targeting Foxo1 in Mice Using Antisense Oligonucleotide Improves Hepatic and Peripheral Insulin Action

Varman T. Samuel,[2] Cheol Soo Choi,[2] Trevor G. Phillips,[2] Anthony J. Romanelli,[2] John G. Geisler,[4] Sanjay Bhanot,[4] Robert McKay,[4] Brett Monia,[4] John R. Shutter,[5] Richard A. Lindberg,[5] Gerald I. Shulman,[1,2,3] and Murielle M. Veniant[5]

Fasting hyperglycemia, a prominent finding in diabetes, is primarily due to increased gluconeogenesis. The transcription factor Foxo1 links insulin signaling to decreased transcription of PEPCK and glucose-6-phosphatase (G6Pase) and provides a possible therapeutic target in insulin-resistant states. Synthetic, optimized antisense oligonucleotides (ASOs) specifically inhibit Foxo1 expression. Here we show the effect of such therapy on insulin resistance in mice with diet-induced obesity (DIO). Reducing Foxo1 mRNA expression with ASO therapy in mouse hepatocytes decreased levels of Foxo1 protein and mRNA expression of PEPCK by 48 ± 4% and G6Pase by 64 ± 3%. In mice with DIO and insulin resistance, Foxo1 ASO therapy lowered plasma glucose concentration and the rate of basal endogenous glucose production. In addition, Foxo1 ASO therapy lowered both hepatic triglyceride and diacylglycerol content and improved hepatic insulin sensitivity. Foxo1 ASO also improved adipocyte insulin action. At a tissue-specific level, this manifested as improved insulin-mediated 2-deoxyglucose uptake and suppression of lipolysis. On a whole-body level, the result was improved glucose tolerance after an intraperitoneal glucose load and increased insulin-stimulated whole-body glucose disposal during a hyperinsulinemic-euglycemic clamp. In conclusion, Foxo1 ASO therapy improved both hepatic insulin and peripheral insulin action. Foxo1 is a potential therapeutic target for improving insulin resistance. *Diabetes* 55: 2042–2050, 2006

From the [1]Howard Hughes Medical Institute, Chevy Chase, Maryland; the [2]Department of Internal Medicine, Yale University School of Medicine, New Haven, Connecticut; the [3]Department of Cellular and Molecular Physiology, Yale University School of Medicine, New Haven, Connecticut; [4]Isis Pharmaceuticals, Carlsbad, California; and [5]Amgen, Thousand Oaks, California.

Address correspondence and reprint requests to Gerald I. Shulman, MD, PhD, TAC S269, P.O. Box 9012, 300 Cedar St., Yale University School of Medicine, New Haven, CT 06510. E-mail: gerald.shulman@yale.edu.

Received for publication 1 June 2005 and accepted in revised form 22 March 2006.

V.T.S. and C.S.C. contributed equally to this work.

J.G.G. is employed by Johnson & Johnson Pharmaceutical Research and Development.

2-DG, 2-deoxyglucose; ASO, antisense oligonucleotide; DAG, diacylglycerol; DIO, diet-induced obesity; EGP, endogenous glucose production; FBS, fetal bovine serum; G6Pase, glucose-6-phosphatase; PPAR, peroxisome proliferator–activated receptor; TG, triglyceride; WAT, white adipose tissue.

DOI: 10.2337/db05-0705

Fasting hyperglycemia, one of the diagnostic criteria for diabetes, is primarily due to increased hepatic gluconeogenesis (1,2). The winged helix transcription factor Foxo1 has been shown to play a pivotal role in the control of gluconeogenesis by linking insulin signaling via AKT2 to decreased transcription of key gluconeogenic enzymes (3–5). Specifically, Foxo1 increases expression of the key gluconeogenic enzymes PEPCK and glucose-6-phosphatase (G6Pase). Insulin-mediated AKT2 phosphorylation of Foxo1 leads to nuclear exclusion, ubiquitination, and degradation (6). The decrease in nuclear Foxo1 subsequently decreases expression levels of PEPCK and G6Pase, decreasing gluconeogenesis and reducing fasting blood glucose. This has been demonstrated in vivo using adenoviral-mediated transfer of a dominant-negative form of Foxo1 into *db/db* mice (7).

Foxo1 has significant roles in extra hepatic tissues. Foxo1-null mice die in utero, suggesting that Foxo1 is involved in coordinating several key components of development (8). Overexpression of Foxo1 in myocytes leads to muscle atrophy (9) and insulin resistance, and overexpression in adipocytes impairs adipocyte differentiation (10). Specifically, Foxo1 coordinates (directly and indirectly) the expression of several genes, including pancreatic duodenal homeobox-1 (11) in β-cells, pyruvate dehydrogenase kinase 4 (12), lipoprotein lipase (13), adiponectin receptors (14) in muscles, and peroxisome proliferator–activated receptor (PPAR)-γ and GLUT4 in adipocytes (10).

The pivotal role of Foxo1 in glucose metabolism makes it an attractive target for pharmacological intervention. Antisense oligonucleotides (ASOs) accumulate and cause reduction of target expression in specific tissues such as liver and fat (but not skeletal or cardiac muscle) and thus may be used to validate therapies disrupting Foxo1 activity. This essentially mimics insulin action at a transcriptional level and may bypass the defects in insulin signaling seen with intracellular lipid accumulation. Reduction of Foxo1 expression is hypothesized to reduce hepatic gluconeogenesis, improve hepatic insulin action, and enhance peripheral insulin-stimulated glucose metabolism. In the present set of studies, we use ASOs to specifically inhibit Foxo1 in lean, insulin-sensitive mice and obese, insulin-resistant mice and assess the subsequent effects on insulin action and glucose metabolism. We performed hyperinsulinemic-euglycemic clamps to assess insulin-stimulated glucose metabolism in liver, muscle, and adipose tissue in mice treated with Foxo1 ASO.

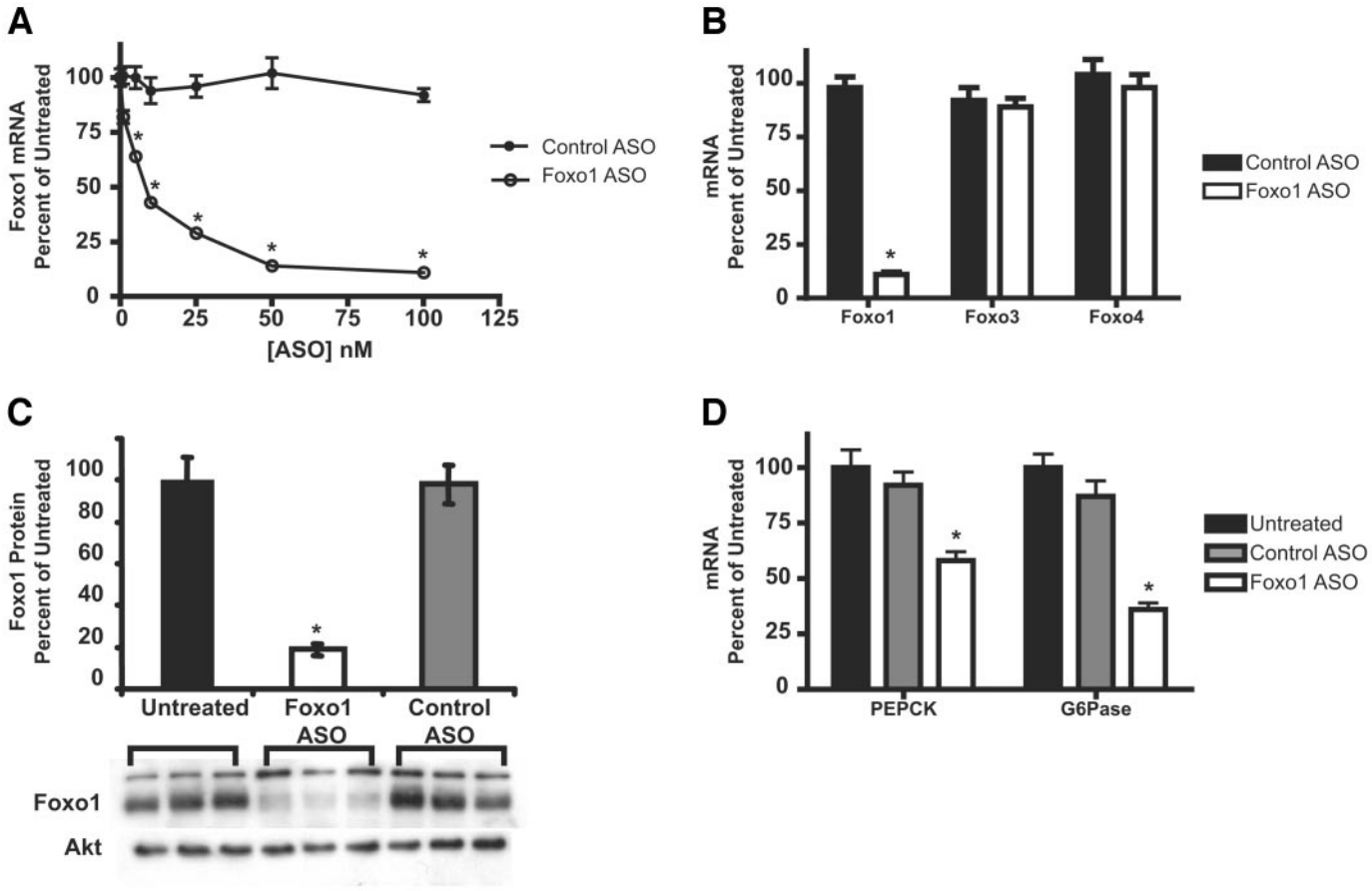

FIG. 1. Effects of Foxo1 ASO in primary mouse hepatocytes. *A*: Foxo1 mRNA expression in cells treated with both control ASO and Foxo1 ASO. *B*: Expression of Foxo1, Foxo3, and Foxo4 mRNA in cells treated with control or Foxo1 ASO. *C*: Foxo1 protein levels assessed by Western blot in untreated cells compared with cells treated with Foxo1 ASO or control ASO. *D*: Expression of PEPCK and G6Pase in untreated cells compared with cells treated with control ASO or Foxo1 ASO. *$P < 0.01$ vs. untreated.

RESULTS

Screening of Foxo1 ASOs in vitro. Eighty ASOs targeting the Foxo1 mRNA were assayed in vitro for their ability to inhibit Foxo1 mRNA expression. This method of screening ASOs has been described previously and produces potent and specific ASOs (15). After extensive dose-response characterization of the most potent ASOs from the screen, one lead ASO, ISIS 188764, was chosen. This ASO sits within the coding region of the Foxo1 mRNA and has no significant cross-reactivity to other Foxo family members. When assayed in a dose-dependent manner in primary mouse hepatocytes, a potent reduction of the Foxo1 mRNA levels was observed (Fig. 1*A*). A control ASO, ISIS 141923, composed of the same chemistry and oligonucleotide length, had no effect on Foxo1 mRNA expression in the same study. This reduction of mRNA levels was specific for Foxo1, as other closely related Foxo family members (Foxo3 and Foxo4) remain unaffected by the ASO treatment (Fig. 1*B*). A significant reduction of Foxo1 protein was seen 48–60 h after ASO treatment (Fig. 1*C*). The kinetics of protein reduction were far longer than that of mRNA reduction (maximal reduction by 6–12 h), due to the time required for previously made protein to decay.

Foxo1 has been established as a key regulator of metabolic gene expression in many in vitro and in vivo model systems, relying mainly on overexpression of normal or mutant forms of Foxo1 protein. To determine if inhibition of endogenous Foxo1 protein with an ASO would have similar gene regulation effects, primary mouse hepatocytes were treated with Foxo1 ASO and then stimulated with glucagon to induce the level of key gluconeogenic genes (Fig. 1*D*). PEPCK and G6Pase-catalytic, two gluconeogenic genes that are critical for hepatic glucose production, were both significantly decreased by Foxo1 ASO treatment. Specifically, there was a 48 ± 4% suppression of PEPCK mRNA and a 64 ± 3% suppression of G6Pase mRNA with Foxo1 ASO treatment compared with 8 ± 6 and 13 ± 7% suppression for PEPCK and G6Pase, respectively, with control ASO treatment (Fig. 1*D*).

Efficacy of Foxo1 ASO in vivo. Chronic high-fat feeding in C57BL/6 mice results in diet-induced obesity (DIO) with hyperglycemia and hyperinsulinemia. In association with these metabolic changes, DIO increased hepatic Foxo1 expression (100 ± 12 vs. 263 ± 40 arbitrary units for lean [$n = 16$] and DIO [$n = 15$], respectively, $P = 0.0005$). The association between insulin resistance and increased Foxo1 expression in mice with DIO provides a model system to test the hypothesis that inhibition of Foxo1 with ASO treatment will improve insulin sensitivity in insulin-resistant states. The design of the treatment course was guided by previous studies and pilot data demonstrating that ASO therapy at 50 mg · kg^{-1} · week^{-1} is both safe and effective in mice. In addition, 3–4 weeks of ASO therapy is required to achieve the maximal stable inhibition of a transcript of interest. In the present set of experiments,

TABLE 1
Transaminase concentrations in lean and DIO mice over 4 weeks of saline, control ASO, or Foxo1 ASO treatment

Group	Week 0	Week 2	Week 4
Lean/saline (IU/ml)			
AST	53 ± 3	62 ± 4	56 ± 3
ALT	32 ± 1	28 ± 2	29 ± 2
DIO/saline (IU/ml)			
AST	115 ± 3	133 ± 9	143 ± 6
ALT	115 ± 10	135 ± 13	133 ± 12
DIO/control ASO (IU/ml)			
AST	119 ± 9	119 ± 10	98 ± 8
ALT	119 ± 15	125 ± 12	132 ± 17
DIO/Foxo1 ASO (IU/ml)			
AST	113 ± 8	107 ± 4	137 ± 11
ALT	113 ± 14	126 ± 9	151 ± 17

Data are means ± SE. ALT, alanine aminotransferase; AST, aspartate aminotransferase.

normal lean and high-fat–fed C57BL/6 mice were treated with Foxo1 ASO for 4–5 weeks to demonstrate that Foxo1 ASO was active in vivo. Within each diet group, there was no difference in body weight between the three treatment arms. Serum transaminase concentrations, as surrogates of hepatotoxicity, over 4 weeks of therapy were not significantly different from basal concentrations (Table 1). While there were dose-dependent decreases in the expression of Foxo1 mRNA, the differences were most marked at the 50-mg · kg^{-1} · $week^{-1}$ dose of Foxo1 ASO (data not shown). As shown in Fig. 2*A*, Foxo1 ASO therapy decreased Foxo1 liver mRNA by 33 ± 6 and 37 ± 6% in both lean and DIO mice, respectively, and Foxo1 fat mRNA by 19 ± 8 and 65 ± 5% (data not shown). This was associated with decreases in hepatic PEPCK in both groups (47 ± 5 and 62 ± 3% for lean and DIO group, respectively) and G6Pase in the lean group (48 ± 4%; Fig. 2*B* and *C*). In contrast, G6Pase expression was not significantly altered by Foxo1 ASO treatment in the DIO group.

Effect of Foxo1 ASO on glucose and insulin concentration. In lean mice, Foxo1 ASO therapy was not associated with any significant change in fed blood glucose levels (Fig. 3*A*); however, it did result in a lowering of plasma insulin levels by 55 ± 9% after 4 weeks of treatment (Fig. 3*C*). In the DIO group, where fed blood glucose level was comparatively higher, Foxo1 ASO therapy led to a significant reduction by 34 ± 3% after 4 weeks of treatment (Fig. 3*B*). Moreover, this reduction in fed-glucose levels occurred with a simultaneous 87 ± 3% reduction in plasma insulin concentration (Fig. 3*D*). Finally, Foxo1 ASO therapy improved clearance of glucose after an intraperitoneal glucose load in both the lean and DIO groups (Fig. 3*E* and *F*). The decreases in glucose and insulin levels and improvements in glucose clearance after a glucose load suggest that inhibition of endogenous Foxo1 affects both hepatic and peripheral insulin action.

Effect of Foxo1 on hepatic insulin action. Discerning the impact of Foxo1 ASO therapy on peripheral and hepatic insulin action was accomplished with hyperinsulinemic-euglycemic clamps. These were performed on 20-week-old mice that were fed either a standard control diet (lean) or a high-fat diet (DIO) for 16 weeks and received saline, control ASO, or Foxo1 ASO therapy twice weekly for 4 weeks. The two diet groups had significantly different weights but, within each diet group, the weights were identical between treatment arms (28.8 ± 0.5 vs. 29.88 ± 0.6 vs. 29.5 ± 0.5 g for lean saline-, control ASO-, and Foxo1 ASO-treated mice, respectively, and 45.8 ± 0.7 vs. 46.8 ± 0.5 vs. 46.2 ± 0.9 g for DIO saline-, control ASO-, and Foxo1 ASO-treated mice, respectively). At the end of the treatment period, the mice underwent a hyperinsulinemic-euglycemic clamp study at 2.5 mU · kg^{-1} · min^{-1} insulin infusion with 2-deoxyglucose (2-DG) infusion to assess tissue-specific glucose uptake. Comparing endogenous glucose production (EGP) under basal and clamped conditions assesses hepatic insulin sensitivity (Fig. 4*A* and *B*). Comparisons of insulin-stimulated whole-body glucose utilization (R_d) and tissue-specific 2-DG uptake provides a complementary assessment of peripheral insulin action. As shown in Fig. 4*B*, compared with the saline and control ASO groups, Foxo1 ASO therapy decreased basal EGP by ~18% in DIO mice (0.48 ± 0.013 vs. 0.48 ± 0.020 vs. 0.41 ± 0.021 mg/min for saline, control, and Foxo1 ASO groups, respectively, $P < 0.05$ vs. saline and control ASO). The decrease in EGP is reflected in the decrease in fasting plasma glucose concentration in the DIO group (107 ± 6.0 vs. 104 ± 4.8 vs. 84 ± 3.2 mg/dl for saline, control, and Foxo1 ASO, respectively, $P < 0.01$ for Foxo1 vs. saline and control). In contrast, neither basal EGP nor basal glucose was affected in the lean group. Under hyperinsulinemic-euglycemic conditions, Foxo1 ASO therapy significantly lowered EGP in the DIO group (Fig. 4*B*, 0.57 ± 0.056 vs. 0.56 ± 0.029 vs. 0.19 ± 0.076 mg/min for saline, control, and Foxo1 ASO, respectively, $P < 0.001$ vs. saline and control ASO).

Previous studies have shown that tissue fat metabolites correlate closely with hepatic insulin resistance. As expected, in comparing the lean and DIO groups, chronic high-fat feeding led to an approximate threefold increase in liver triglyceride (TG) content. As seen in Fig. 4*C*, Foxo1 ASO therapy did not alter liver TG content in the lean group (20 ± 4 vs. 17 ± 4 vs. 14 ± 3 mg/g liver for saline, control ASO, and Foxo1 ASO, respectively, ANOVA $P = 0.58$). In contrast, in the DIO group, Foxo1 ASO therapy normalized liver TG content to nearly that of the lean group (Fig. 4*D*, 46 ± 2 vs. 65 ± 11 vs. 23 ± 4 mg/g for saline, control ASO, and Foxo1 ASO, respectively, $P < 0.01$ for control ASO vs. Foxo1 ASO). This decrease in liver TG occurred in the absence of any significant differences in body weight or percent fat mass as assessed by ^{1}H magnetic resonance spectroscopy (43.4 vs. 45.5 vs. 45.0% for saline, control ASO, and Foxo1 ASO, respectively). The fat metabolites were further analyzed by LC/MS/MS (liquid chromatography/mass spectrometry/mass spectrometry) to distinguish differences in diacylglycerol (DAG) and fatty acyl CoA species (Fig. 4*E*). Hepatic DAG content mirrored hepatic TG content. The expected increase in DAG concentration with high-fat feeding was reversed with Foxo1 ASO treatment (Fig. 4*E*). The total DAG contents in the lean group were 18.6 ± 2.6 vs. 13.1 ± 3.7 vs. 11.0 ± 0.6 μmol/g liver (ANOVA $P = 0.16$) for the saline, control ASO, and Foxo1 ASO, respectively. The total DAG content for the DIO group was 32.1 ± 3.3 vs. 32.5 ± 4.7 vs. 12.9.2 ± 4.1 μmol/g liver (Fig. 4*E*, *inset*) for the saline, control ASO, and Foxo1 ASO groups, respectively ($P < 0.05$ vs. saline and <0.01 vs. control ASO). In analyzing the profile of the constituent DAGs, the DIO group showed a predominance of DAG species containing oleic acid (i.e., OO and OL) and palmitic acid (i.e., PL). This reflects the predominance of oleic acid and palmitic acid in lard, the major dietary fat provided to the DIO mice. The concentration for most of

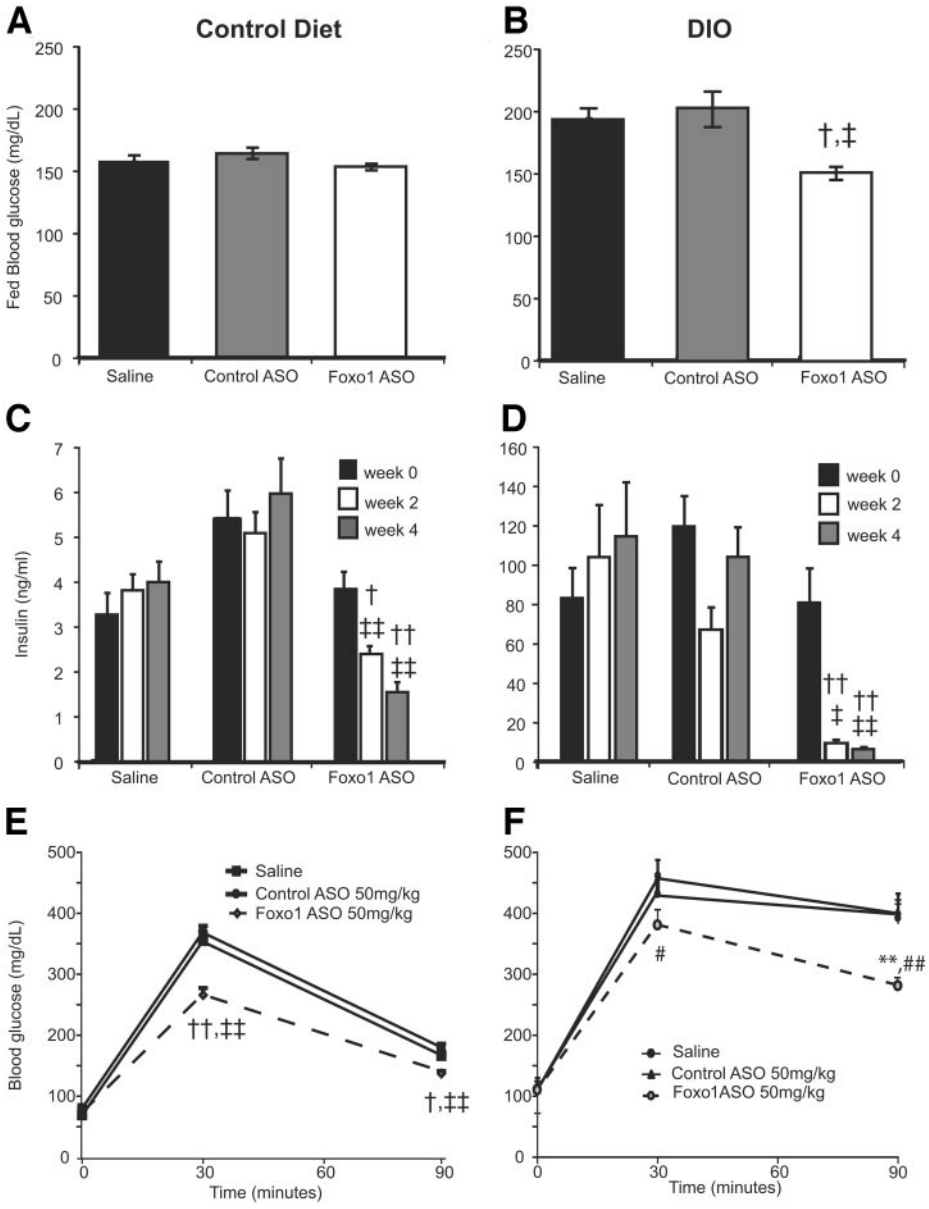

FIG. 2. Effects of Foxo1 ASO on gene transcription in lean and DIO mice. Mice were treated for 4 weeks with saline, control ASO, or Foxo1 ASO at a dose of 50 mg · kg^{-1} · week^{-1}. *A*: Expression of Foxo1 mRNA. *B*: Expression of PEPCK mRNA. *C*: Expression of G6Pase (catalytic subunit) mRNA. **P* < 0.05 vs. saline; †*P* < 0.01 vs. saline; ‡*P* < 0.01 vs. control ASO; ***P* < 0.001 vs. saline; ##*P* < 0.001 vs. control ASO.

the DAG species measured was decreased with Foxo1 ASO. In contrast to TG and DAG, chronic high-fat feeding did not increase fatty acyl CoA content. For the lean mice, total hepatic fatty acyl CoA content was 115.1 ± 21.7 vs. 141.2 ± 21.4 vs. 75.5 ± 15.5 nmol/g liver for saline, control ASO, and Foxo1 ASO, respectively (ANOVA $P = 0.12$). In the DIO group, total fatty acyl CoA content was 88.7 ± 14.9 vs. 90.4 ± 18.7 vs. 102.7 ± 22.8 nmol/g for saline, control ASO, and Foxo1 ASO, respectively (ANOVA $P = 0.84$). Thus, chronic high-fat feeding led to increases in hepatic TG and DAG (but not fatty acyl CoA) that were reversed with Foxo1 ASO treatment.

Effect of Foxo1 on peripheral insulin action. Measuring the rate of insulin-mediated whole-body R_d and tissue-specific 2-DG uptake reveals the effects of Foxo1 ASO on peripheral insulin action. As expected, peripheral glucose metabolism was decreased in the DIO group compared with lean mice. As shown in Fig. 5*A*, there was no difference in peripheral glucose metabolism between saline-treated or control ASO–treated mice in either lean (1.16 ± 0.06 vs. 1.14 ± 0.06 for saline and control ASO, respectively) or DIO (0.94 ± 0.03 vs. 0.82 ± 0.04 mg · kg^{-1} · min^{-1} for saline and control ASO, respectively) mice. Foxo1 ASO therapy resulted in modest improvements in peripheral glucose metabolism in both diet groups, although this difference only achieved statistical significance in the DIO group. To better understand the mechanism for the increased peripheral glucose metabolism, tissue-specific 2-DG uptake was measured. There was no statistically significant difference in gastrocnemius 2-DG (Fig. 5*B*) from either the lean (53.3 ± 5.84 vs. 54.7 ± 7.35 vs. 67.2 ± 2.77 mg · kg^{-1} · min^{-1} for saline, control ASO, and Foxo1 ASO, respectively, ANOVA $P = 0.16$) or DIO (57.7 ± 7.14 vs. 40.8 ± 4.46 vs. 46.0 ± 3.89 mg · kg^{-1} · min^{-1} for saline, control ASO, and Foxo1 ASO, respectively, ANOVA $P = 0.09$) groups. In contrast, as shown in Fig. 5*C*, Foxo1 ASO therapy improved epididymal white adipose tissue (WAT) glucose uptake in both the lean (3.28 ± 0.58 vs. 3.69 ± 0.66 vs. 7.66 ± 0.93 mg · kg^{-1} · min^{-1} for saline, control, and Foxo1 ASO, respectively, $P < 0.01$ compared with saline and control ASO) and DIO (5.94 ± 0.96 vs. 6.86 ± 0.68 vs. 8.82 ± 0.53 mg · kg^{-1} ·

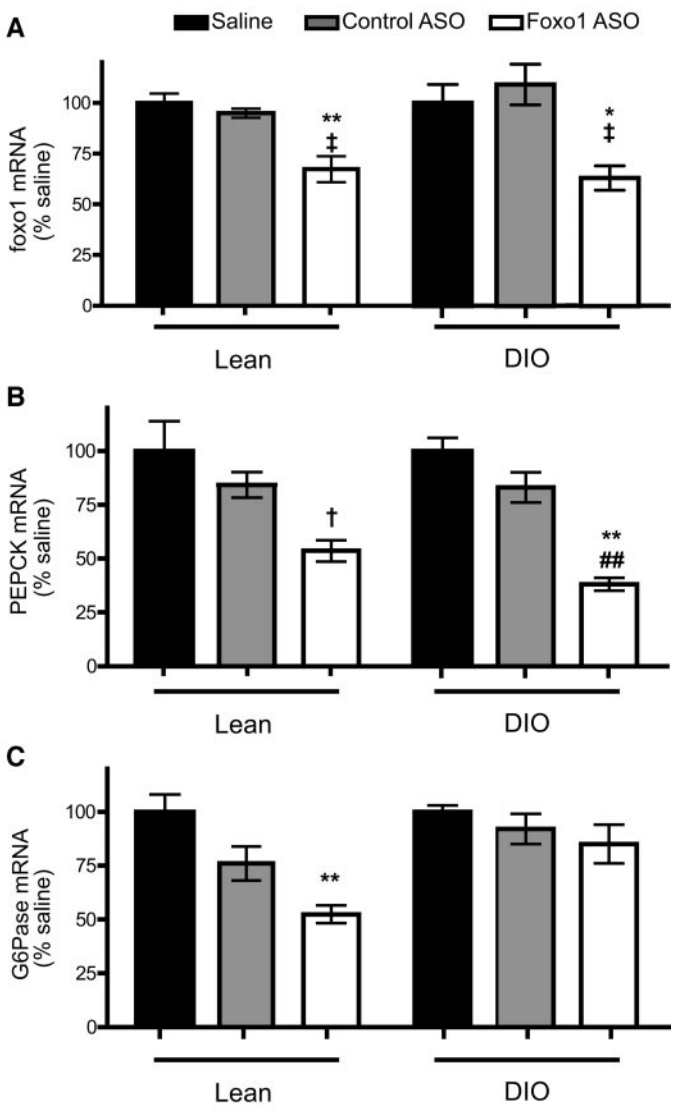

FIG. 3. Effects of Foxo1 ASO on glucose and insulin values in lean (*A*, *C*, and *E*) and obese (DIO; *B*, *D*, and *F*) mice. *A*: Fed blood glucose concentration in lean mice. *B*: Fed glucose levels in DIO mice treated with saline, control ASO, or Foxo1 ASO. †$P < 0.01$ vs. saline; ‡$P = 0.01$ vs. control. *C*: Fed insulin levels in lean mice over 4 weeks of therapy. *D*: Fed insulin levels in DIO mice over 4 weeks of therapy. †$P < 0.01$ vs. saline; ††$P < 0.0001$ vs. saline; ‡‡ $P < 0.001$ vs. control. *E*: Intraperitoneal glucose load in lean mice treated with saline, control ASO, or Foxo1 ASO. *F*: Intraperitoneal glucose load in DIO mice treated with saline, control ASO, or Foxo1ASO. †$P = 0.0013$ vs. saline; **$P \leq 0.001$ vs. saline; ††$P < 0.0001$ vs. saline; #$P < 0.05$ vs. control; ##$P = 0.004$ vs. control.

min^{-1} for saline, control, and Foxo1 ASO, respectively, $P < 0.05$ vs. saline; $P = 0.13$ vs. control ASO) mice. The ability of insulin to suppress peripheral lipolysis and decrease fatty acid concentration also serves as an indicator of adipose insulin sensitivity. The decrease in the ability of insulin to suppress fatty acid concentration seen in the DIO group was partially reversed by Foxo1 ASO therapy in the DIO group (23.4 ± 5.9 vs. 20.9 ± 5.3 vs. 30.8 ± 8.2% for saline, control ASO, and Foxo1 ASO, respectively, in lean mice and 10.2 ± 6.60 vs. 2.4 ± 5.0 vs. 30.9 ± 6.24% suppression for saline, control ASO, and Foxo1 ASO, respectively, for DIO mice, $P < 0.01$ vs. control ASO; Fig. 5*D*). In summary, Foxo1 ASO therapy was associated with modest improvements in peripheral insulin action that appear to largely be accounted for by increases in adipose insulin sensitivity.

DISCUSSION

Insulin-mediated phosphorylation of Foxo1, via AKT2, leads to Foxo1 nuclear exclusion and degradation. Therefore, reducing Foxo1 mRNA expression using specific ASOs should echo insulin action at a transcriptional level. Reduction of Foxo1 expression has the potential to remedy many of the defects seen in insulin-resistant states by mimicking insulin action in the nucleus despite acquired cytoplasmic defects in the insulin signaling cascade. The studies presented in this manuscript validate the therapeutic potential for Foxo1 inhibition in two key insulin-target tissues (liver and adipose tissue) and quantitate this effect. First, ASOs designed against Foxo1 lower Foxo1 mRNA and protein levels and, in turn, lower expression of gluconeogenic enzymes. Second, these changes lower endogenous glucose production and, as a consequence, lower glucose and insulin concentrations. Third, Foxo1 ASO therapy normalized hepatic lipid concentration in DIO mice and improved hepatic insulin action. Finally, Foxo1 ASO therapy improved insulin-stimulated white adipocyte glucose uptake without any discernible effect on muscle glucose uptake.

From a pool of ~80 synthetic oligonucleotides designed against Foxo1 mRNA, a single-lead ASO was chosen for in vivo studies based on its potency in both in vitro and in vivo screens. In vitro, this ASO demonstrated a dose-dependent decrease in Foxo1 mRNA and Foxo1 protein levels without any change in the expression of Foxo3 and Foxo4, two related transcription factors. Moreover, the decrease in Foxo1 mRNA was associated with a decrease in PEPCK and G6Pase mRNA expression. This same ASO was tested in two relevant mouse models, one lean and one obese (DIO).

Interestingly, with DIO, there was an increase in Foxo1 mRNA and protein levels in the liver. The mechanism for this increase with fat feeding is not clear but suggests an association between diet-induced insulin resistance and increases in Foxo1. Treatment with Foxo1 ASO at a dose of 50 $mg \cdot kg^{-1} \cdot week^{-1}$ led to a 20–40% decrease in Foxo1 mRNA levels. Physiologically, Foxo1 inhibition markedly decreased fasting insulin in the DIO group with a ~15% decrease in the rate of EGP and ~20% decrease in fasting plasma glucose. This decrease in EGP and fasting glucose appears to be primarily achieved by the 50% decrease in PEPCK without any significant suppression of G6Pase. These findings demonstrate that a proximal block in the gluconeogenic pathway is sufficient to decrease EGP and lower fasting plasma glucose. The finding that G6Pase expression was not significantly altered in DIO mice treated with Foxo1 ASO suggests that other factors (i.e., HNF4, glucocorticoids, LXR) may eclipse Foxo1 inhibition in driving G6Pase transcription.

In addition to the changes in basal hepatic glucose metabolism, Foxo1 ASO therapy improved hepatic insulin sensitivity. The present data show that Foxo1 ASO treatment resulted in a nonsignificant trend toward increased suppression of EGP in the lean group (~25%) and a significant suppression of EGP by 50% in the DIO group. One possible explanation for the increased hepatic insulin responsiveness seen with Foxo1 ASO treatment in the DIO group is that the lowering of intrahepatic lipid content improved hepatic insulin action. Previous studies have

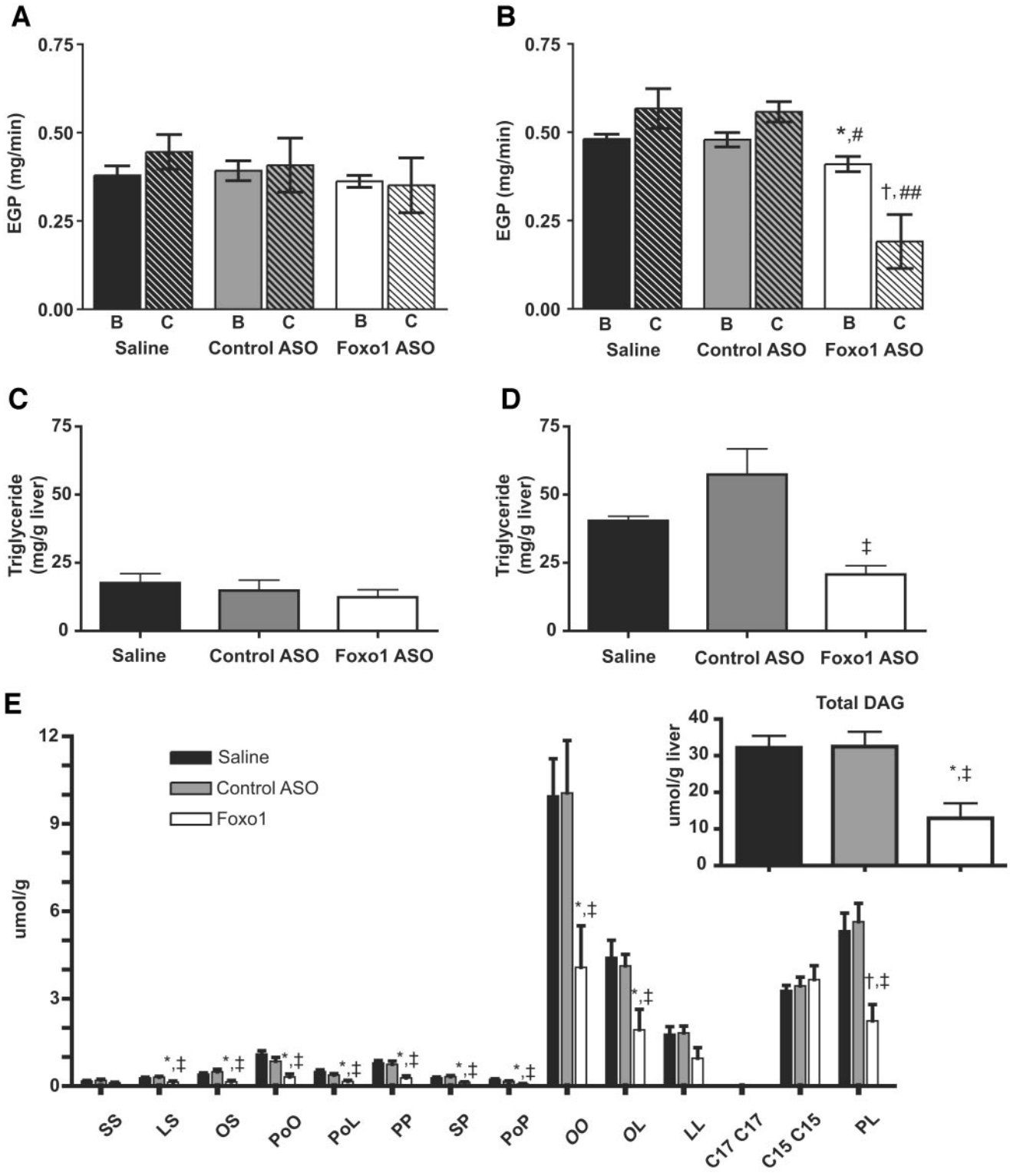

FIG. 4. Foxo1 ASO alters hepatic glucose and fat metabolism. *A* and *B*: Effects of Foxo1 ASO on hepatic glucose output under basal (B) and hyperinsulinemic-euglycemic clamp (C) conditions in lean (*A*) and DIO (*B*) mice. **P* < 0.05 vs. saline/basal; #*P* < 0.05 vs. control/basal; †*P* < 0.01 vs. saline/clamped; ##*P* < 0.01 vs. control ASO/clamped. *C* and *D*: Hepatic TG content in lean (*C*) and DIO (*D*) mice (‡*P* < 0.01 vs. control ASO). *E*: Hepatic diacylglycerol species in DIO mice treated with saline, control ASO, or Foxo1 ASO. Each bar represents the mean for the treatment group ± SE. Inset represents mean total DAG content for each treatment group ± SE. **P* < 0.05 vs. saline; †*P* < 0.01 vs. saline; ‡*P* < 0.01 vs. control ASO.

shown that changes in intrahepatic fat content correlate inversely with hepatic insulin action (16–21). In the present study, Foxo1 ASO therapy decreased hepatic TG and DAG content in the DIO mice to levels approaching those of the lean mice and, as a consequence, improved hepatic insulin action.

Foxo1 inhibition led to modest improvements in peripheral insulin action as well. Foxo1 ASO therapy decreased

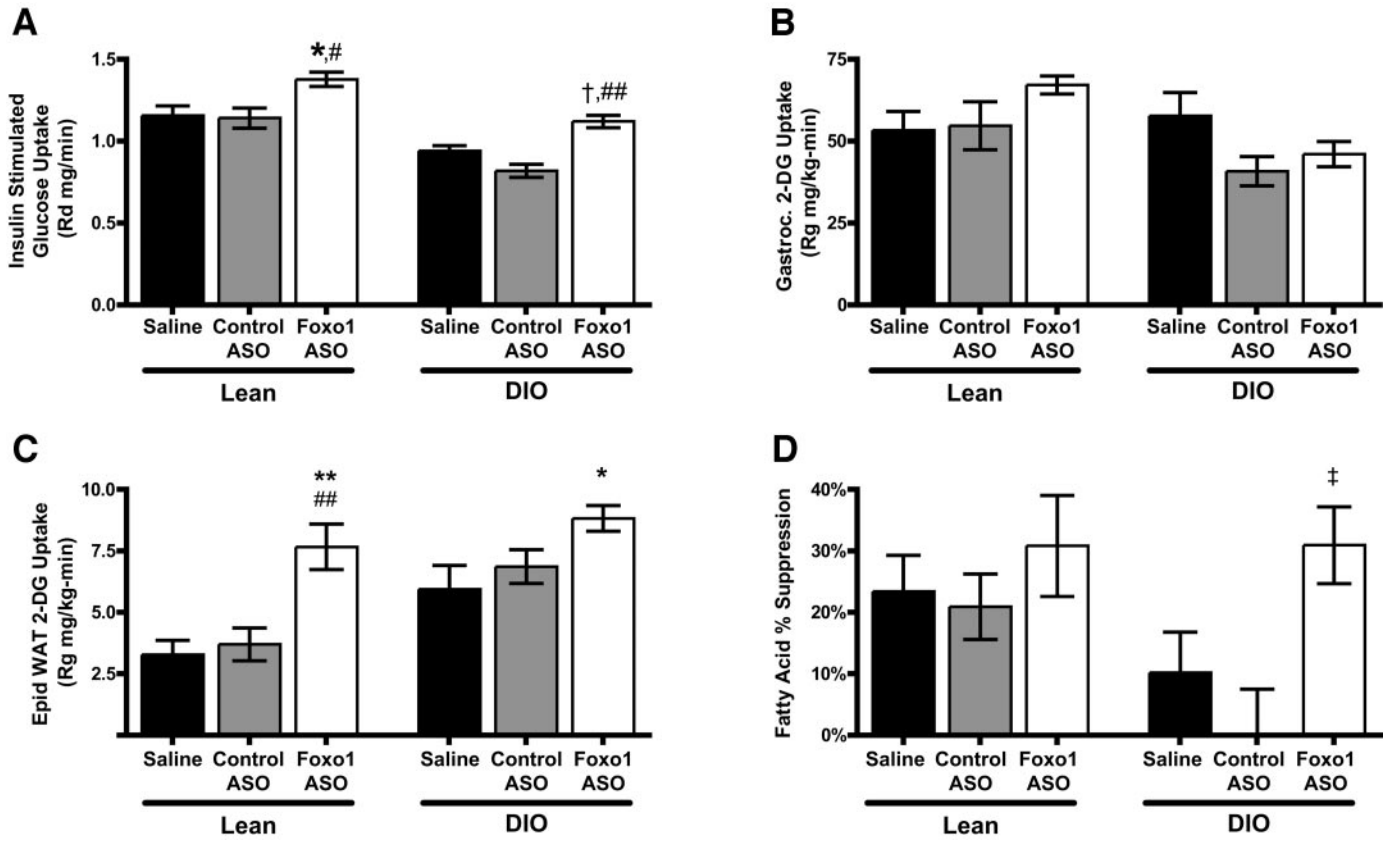

FIG. 5. Peripheral insulin action in lean and DIO mice treated with saline, control ASO, or Foxo1 ASO. *A*: Effect of Foxo1 ASO on whole-body insulin-mediated glucose uptake (R_d). *B*: Gastrocnemius 2-DG uptake. *C*: Epididymal WAT 2-DG uptake. *D*: Suppression of plasma fatty acid during hyperinsulinemic-euglycemic clamp. *$P < 0.05$ vs. saline; #$P < 0.05$ vs. control ASO; †$P < 0.01$ vs. saline; ‡$P < 0.01$ vs. control ASO; **$P = 0.001$ vs. saline; ##$P = 0.003$ vs. control ASO.

the excursion of blood glucose in response to an intraperitoneal glucose load, suggesting improved whole-body clearance of glucose. This was confirmed with the hyperinsulinemic-euglycemic clamp, where Foxo1 ASO therapy increased peripheral glucose metabolism by ~15% in the lean group and ~20% in the DIO group. Finally, in analyzing tissue-specific 2-DG uptake, there was ~40% and ~100% increase in epididymal WAT glucose uptake with Foxo1 ASO therapy in the DIO and lean groups, respectively. Foxo1 ASO therapy nearly normalized the impaired insulin-stimulated WAT glucose uptake in the DIO group. Dowell et al. (22) described an antagonistic relationship between Foxo1 and PPAR-γ where Foxo1 decreased the formation of a PPAR-γ/RXR/DNA complex. Therefore, reducing Foxo1 mRNA expression may lead to improvements in PPAR-γ activity. However, in the present study, the expression of PPAR-γ target genes (*aP2*, *ACS*, and *FATP*) in epididymal adipose tissue was unaffected by Foxo1 ASO treatment, suggesting that other mechanisms may be at work (data not shown). The absence of any improvements in muscle insulin action may reflect the ability of ASOs to accumulate in liver and adipose as opposed to muscle (23). Thus, Foxo1 ASO therapy results in modest improvements in peripheral insulin action, mainly through improvements in adipose tissue insulin response, which may be a result of improved PPAR-γ activity.

These results are consistent with previous studies by Nakae et al. (24), in which Foxo1 haploinsufficient mice were crossed with mice lacking the insulin receptor, and by Altomonte et al. (7), in which *db/db* mice were treated with an adenovirus expressing a dominant-negative mutant of Foxo1. In both studies, decreasing Foxo1 action lowered levels of PEPCK and G6Pase mRNA and lowered blood glucose concentration. The present set of studies build on this previous work by measuring organ-specific insulin action and quantifying changes in glucose flux in mice made insulin resistant by chronic high-fat feeding. First, DIO is associated with elevations in hepatic Foxo1. Second, modest inhibition (~40% knockdown) of endogenous Foxo1 is sufficient to lower basal EGP and blood glucose and insulin levels and improve hepatic insulin action under hyperinsulinemic conditions. Finally, Foxo1 inhibition also improved adipocyte insulin action. While we were unable to detect any significant differences in the expression key genes (adipose tissue GLUT4, adiponectin, adiponectin receptor, and tumor necrosis factor-α), we did measure increases in insulin-stimulated glucose uptake and suppression of lipolysis. In conclusion, the studies here support the hypothesis that therapies aimed at reducing endogenous Foxo1 expression will improve glucose homeostasis in insulin-resistant states. Moreover, the salutary effects of Foxo1 extend beyond its ability to reduce EGP and include a reduction of hepatic steatosis and an increase in adipocyte insulin responsiveness.

RESEARCH DESIGN AND METHODS

All mice were maintained in accordance with the institutional Animal Use and Care Committees of Amgen and Yale University School of Medicine. C57BL/6 mice were obtained at 3–4 weeks of age from Charles River Laboratories

(Wilmington, MA) and acclimated for 1 week after arrival and before initiation of the experiment. Mice received food and water ad libitum and were maintained on a 12:12-h light-dark cycle (lights on at 6:30 A.M.). Mice were housed five per cage for the first 8 weeks of the feeding regimen and single-housed for 4 weeks before initiation of treatment. From a cohort of 100 mice, 80 were started on a high-fat diet (Research Diets D12492) at 3 weeks of age for 12 weeks. The remaining 20 mice were kept on a normal rodent diet. Body weight was monitored, and mice were randomized on blood glucose values and body weight before starting the treatment. Blood samples (~150 μl) were collected by retroorbital bleed into EDTA plasma tubes before the initiation of the ASO or saline treatment of each study and every other week after the treatment was started. Blood glucose was measured using a OneTouch Profile glucometer (LifeScan, Milpitas, CA). All ASOs (control and Foxo1) were prepared in normal saline, and the solutions were sterilized through a 0.2-μm filter. Mice in each diet group were dosed with ASO solutions or saline twice per week via intraperitoneal injection at a dose of 50 $mg \cdot kg^{-1} \cdot week^{-1}$. This dose was chosen on the basis of pilot studies showing it to the be most efficacious, nontoxic dose with regards to suppression of Foxo1 mRNA. During the treatment period, body weight and food intake were measured weekly.

Selection of murine Foxo1 ASO. Rapid-throughput screens were performed in vitro to identify a murine Foxo1-selective ASO inhibitor as previously described (15). In brief, 80 ASOs were designed to the mouse Foxo1 mRNA sequence. All ASOs were synthesized as 20-base phosphorothioate chimeric ASOs, where bases 1–5 and 16–20 were modified with 2′-O-(2-methoxy)-ethyl. This chimeric design has been shown to provide both increased nuclease resistance and mRNA affinity, while maintaining the robust RNase H terminating mechanism utilized by these types of ASOs (25). These benefits result in an attractive in vivo pharmacological and toxicological profile for 2′-O-(2-methoxy)-ethyl chimeric ASOs. The ASOs were screened in mouse primary hepatocytes for their ability to inhibit Foxo1 mRNA expression. The final-lead mouse Foxo1 ASO, ISIS 188764, was selected after detailed characterization in vitro and in silico. ISIS 188764 has the sequence 5′-TCCAGTTCCTTCATTCTGCA-3′ and hybridizes to position 10961-115 on Genbank accession no. AJ252157.1. The control ASO, ISIS 141923, has the sequence 5′-CCTTCCCTGAAGGTTCCTCC-3′ and does not have perfect complementarity to any known gene in public databases.

In vitro treatment of primary hepatocytes with Foxo1 ASOs. Primary murine hepatocytes were isolated, as previously described, and plated onto collagen-coated plates (26). Hepatocytes were treated with ASO and Lipofectin (Invitrogen) mixture for 4 h in serum-free William's E media (Invitrogen). ASO and Lipofectin were mixed at a ratio of 3 μg Lipofectin for every 1 ml of 100-nmol/l ASO concentration. After 4 h, ASO reaction mixture was replaced with normal maintenance media (William's E media with 10% fetal bovine serum [FBS]) and the cells incubated under normal conditions for indicated times (generally, 20–24 h for RNA and 60 h for protein).

Analysis of Foxo1 mRNA from in vitro samples. Total RNA was extracted from cells using the RNeasy 96-kit (Qiagen, Valencia, CA) as per manufacturer's protocol. RT-PCR analysis of Foxo1 and other mRNAs was performed using an ABI Prism 7700 Sequence Detector (Applied Biosystems, Foster City, CA) as described previously (27). Briefly, 100 ng total RNA was analyzed in a final volume of 25 μl containing 200 nmol/l gene-specific PCR primers, 0.2 mmol/l each dNTP, 75 nmol/l fluorescently labeled oligonucleotide probe, 1× RT-PCR buffer, 5 mmol/l $MgCl_2$, 2 units Platinum *Taq*DNA polymerase (Invitrogen), and 8 units ribonuclease inhibitor. Reverse transcription was performed for 30 min at 48°C followed by PCR: 40 thermal cycles of 30 s at 94°C and 1 min at 60°C. All expression data were normalized to a Ribogreen (Molecular Probes) value, which is a measurement of total RNA. Primer-probe sets were synthesized by IDT (Coralville, IA), with the probes synthesized with FAM-TAM fluorophores. The following primer-probe sets were used for mRNA expression analysis: Foxo1: forward primer CAAAGTACACATACGGC CAATCC, reverse primer CGTAACTTGATTTGCTGTCCTGAA, probe TGAGC CCTTTGCCCCAGATG CCTAT. Foxo3: forward primer AACAGACCAGCCAC CTTCTCTT, reverse primer TGAAGCAAGCAGGTCTTGGA, probe CGTGTCA CACTACGGCAA CCAGACA. Foxo4: forward primer ATGCTGTTGGAAATGT GAAGTCA, reverse primer CTCAGCTCAGATAAGACTCTCTACAAAAA, probe TGGCCTTACCCCTGCCTTTG.

Analysis of Foxo1 protein by Western blot. Total cellular protein was extracted from cells by lysing cells at 4°C with protein extraction buffer (10 mmol/l Tris, pH 7.4, 150 mmol/l NaCl, 2 mmol/l EDTA, 5 mmol/l EGTA, 1% Triton X-100, 0.5% NP-40, 1 mmol/l sodium orthovanadate, 1 mmol/l NaF, and protease inhibitor cocktail tablet [Complete; Roche Diagnostics, Indianapolis, IN]). Extracts were centrifuged at 14,000*g* at 4°C for 10 min and supernatant saved as total protein lysate. Protein was quantitated using a modified Lowry assay (DC protein assay; Bio-Rad, Hercules, CA). For Western blot detection of individual proteins, 20–40 μg total protein lysate was electrophoresed through 8% Tris-Glycine polyacrylamide gels (Invitrogen, Carlsbad, CA) and then transferred to nylon membrane (Immobilon-P; Millipore, Billerica, MA). Membranes were blocked in 5% nonfat milk (Bio-Rad) for 1 h and then incubated with primary antibody overnight at 4°C. Antibodies used were Foxo1 (0.25 μg/ml, 07-176; UBI) and Akt (1:1,000, 9272; Cell Signaling). Membranes were washed with Tris-buffered saline and then incubated with horseradish peroxidase anti-rabbit secondary antibody (1:2,000; UBI) for 1 h. After extensive washing, proteins were visualized using ECL-Plus kit (Amersham, Piscataway, NJ) per the manufacturer's protocol. Membranes were either exposed to film or scanned (Typhoon Scanner; Molecular Dynamics [Amersham Biosciences], Piscataway, NJ) and then quantitated using ImageQuant software.

In vitro modulation of metabolic gene expression. Primary mouse hepatocytes were treated with ASO, as described above, and then incubated in normal maintenance (William's E with 10% FBS) media for 48 h. Cells were then incubated in William's E with 0.1% FBS for 12 h, followed by a 1-nmol/l glucagon (Sigma, St. Louis, MO) stimulation for 4 h. RNA was extracted as described above, followed by analysis of metabolic gene expression with RT-PCR as described above. Primer-probe sets were synthesized as described above. PEPCK: forward ATCCAGGGCAGCCTCGA, reverse AGCATTGCC TTCC ACGAACT, probe AGCCTGCCCCAGGCAGTGAGG; G6Pase-catalytic: forward TGCAAGGGAGAACTCAGCAA, reverse GGACCAAGGAAGCCACA ATG, probe TCGTTCCCATTCCGCTTCGCC; FASn: forward CATGACCTCG TGAT GAACGTGT, reverse CGGGTGAGGACGTTTACAAAG, probe CCGT CACT TCCAGTTAGAGCAGGACAAGC.

Glucose tolerance test. Mice were fasted from 9:00 P.M. to 9:00 A.M. Blood glucose was measured at 9:00 A.M., and an intraperitoneal glucose bolus (2 g/kg body wt) was administered to conscious, unrestrained mice. Blood glucose was measured at 30 and 90 min after glucose injection using a OneTouch Profile glucometer. To minimize stress levels, 60- and 120-min glucose levels were not measured.

Hyperinsulinemic-euglycemic clamp studies. Four days before the hyperinsulinemic-euglycemic studies, mice had body composition assessed by ^1H magnetic resonance spectroscopy (Bruker BioSpin, Billerica, MA). Jugular venous catheters were implanted and the mice allowed to recover for 4 days. After an overnight fast, [3-^{3}H]glucose (HPLC purified; Perkin Elmer, Boston, MA) was infused at a rate of 0.05 μCi/min for 2 h to assess the basal glucose turnover. Following the basal period, the hyperinsulinemic-euglycemic clamp was conducted for 120 min with a primed/continuous infusion of human insulin (300-pmol/kg prime, 15-$pmol \cdot kg^{-1} \cdot min^{-1}$ infusion) (Novo Nordisk, Princeton, NJ) and a variable infusion of 20% dextrose to maintain euglycemia (~100–120 mg/dl). Plasma samples were obtained from the tail at 20, 40, 55, 70, 75, 80, 95, and 120 min [3-^{3}H]glucose was infused at a rate of 0.1 μCi/min throughout the clamps and 2-deoxy-D-[1-^{14}C]glucose (DOG; Perkin Elmer) was injected as bolus at the 75th min of the clamp to estimate the rate of insulin-stimulated tissue glucose uptake as previously described (28). At the end of clamp, mice were anesthetized with pentobarbital sodium injection (150 mg/kg), and all tissues were taken within 4 min, frozen immediately using liquid N_2-cooled aluminum tongs, and stored at −80°C for later analysis.

Biochemical analysis and calculations. Plasma glucose was analyzed during the clamps using 10 μl plasma by a glucose oxidase method on a Beckman glucose analyzer II (Beckman, Fullerton, CA). Plasma insulin was measured by radioimmunoassay using a kit from Linco Research (St. Charles, MO). Plasma free fatty acid was determined using an acyl-CoA oxidase–based colorimetric kit (Wako Pure Chemical Industries, Osaka, Japan). For the determination of plasma ^{3}H-glucose and ^{14}C-2-DG, plasma was deproteinized with $ZnSO_4$ and $Ba(OH)_2$, dried to remove ^3H_2O, resuspended in water, and counted in scintillation fluid (Ultima gold; Perkin Elmer) on a Beckman scintillation counter.

Rates of basal and insulin-stimulated whole-body glucose turnover were determined as the ratio of the [3-^{3}H]glucose infusion rate (disintegrations per minute [dpm] per minute) to the specific activity of plasma glucose (dpm per mg) at the end of basal period and during the final 30 min of clamp experiment, respectively. Hepatic glucose output was determined by subtracting the glucose infusion rate from the total glucose appearance. For the determination of individual tissue glucose uptake, tissue samples were homogenized and the supernatants subjected to an ion-exchange column to separate tissue ^{14}C-2-DG-6-phosphate from ^{14}C-2-DG. Tissue glucose uptake was calculated from area under curve of plasma ^{14}C-2-DG profile and muscle ^{14}C-2-DG-6-phosphate content, as previously described (28).

Tissue lipid measurement. The solid-phase extraction and purification of medium, long-chain, and very-long-chain fatty acyl-CoAs from liver have been described previously (29,30). After purification, fatty acyl-CoA fractions were dissolved in methanol/H_2O (1:1 [vol/vol]) and subjected to LC/MS/MS analysis. A turbo ionspray source was interfaced with an API 3000 tandem mass spectrometer (Applied Biosystems) in conjunction with two Perkin Elmer 200 Series micro pumps and a 200 Series autosampler (Perkin Elmer, Norwalk, CT). The transition pairs [M-2H]2-:[M-H-80]- (Q1 and Q3) were monitored in

negative multiple reaction monitor mode for each fatty acyl-CoA species. Total fatty acyl-CoA content is expressed as the sum of individual species. The DAG extraction was performed as previously described (31). An aliquot of the organic phase was retained for measurement of TG content. This was passed over preconditioned columns (Sep-Pak Cartridge WAT020845; Waters, Milford, MA) to purify the DAG component. Using mass spectrometry the transition pairs [M+H-18]+: fatty acids from DAG (Q1 and Q3) were monitored in positive multiple reaction monitor mode for each DAG metabolite. Total DAG content is expressed as the sum of individual species. Tissue TG was extracted using the method of Bligh and Dyer (29) and measured using a DCL Triglyceride Reagent (Diagnostic Chemicals Limited, Charlottetown, Prince Edward Island, Canada).

Statistical analyses. All values are expressed as the means ± SE. Comparisons across the three groups were done using one-way ANOVA. When the ANOVA yielded a significant difference, post hoc analysis was done using Tukey's honestly significant difference test.

ACKNOWLEDGMENTS

This work was supported by grants from the U.S. Public Health Service (K23 RR-17404 to V.T.S., R01 DK-40936 to G.I.S., and P30 DK-45735 to G.I.S.), Amgen, and a Distinguished Clinical Scientist Award from the American Diabetes Association. T.G.P. was a Howard Hughes Medical Institute Clinical Research Fellow. G.I.S. is an investigator of the Howard Hughes Medical Institute.

We thank Renee Komorowski for her pharmacological expertise and Jocelyn McCormick, Shanaka Stanislaus, Liying Deng, Rod Cupples, and Dr. Jason Kim for their assistance.

REFERENCES

1. Hwang JH, Perseghin G, Rothman DL, Cline GW, Magnusson I, Petersen KF, Shulman GI: Impaired net hepatic glycogen synthesis in insulin-dependent diabetic subjects during mixed meal ingestion: a 13C nuclear magnetic resonance spectroscopy study. *J Clin Invest* 95:783–787, 1995
2. Hundal R, Krssak M, Dufour S, Laurent D, Lebon V, Chandramouli V, Inzucchi SE, Schumann WC, Petersen KF, Landau BR, Shulman GI: Mechanism by which metformin reduces glucose production in type 2 diabetes. *Diabetes* 49:2063–2069, 2000
3. Nakae J, Kitamura T, Silver DL, Accili D: The forkhead transcription factor Foxo1 (Fkhr) confers insulin sensitivity onto glucose-6-phosphatase expression. *J Clin Invest* 108:1359–1367, 2001
4. Nakae J, Kitamura T, Ogawa W, Kasuga M, Accili D: Insulin regulation of gene expression through the forkhead transcription factor Foxo1 (Fkhr) requires kinases distinct from Akt. *Biochemistry* 40:11768–11776, 2001
5. Puigserver P, Rhee J, Donovan J, Walkey CJ, Yoon JC, Oriente F, Kitamura Y, Altomonte J, Dong H, Accili D, Spiegelman BM: Insulin-regulated hepatic gluconeogenesis through FOXO1-PGC-1alpha interaction. *Nature* 423:550–555, 2003
6. Matsuzaki H, Daitoku H, Hatta M, Tanaka K, Fukamizu A: Insulin-induced phosphorylation of FKHR (Foxo1) targets to proteasomal degradation. *Proc Natl Acad Sci U S A* 100:11285–11290, 2003
7. Altomonte J, Richter A, Harbaran S, Suriawinata J, Nakae J, Thung SN, Meseck M, Accili D, Dong H: Inhibition of Foxo1 function is associated with improved fasting glycemia in diabetic mice. *Am J Physiol Endocrinol Metab* 285:E718–E728, 2003
8. Hosaka T, Biggs WH 3rd, Tieu D, Boyer AD, Varki NM, Cavenee WK, Arden KC: Disruption of forkhead transcription factor (FOXO) family members in mice reveals their functional diversification. *Proc Natl Acad Sci U S A* 101:2975–2980, 2004
9. Kamei Y, Miura S, Suzuki M, Kai Y, Mizukami J, Taniguchi T, Mochida K, Hata T, Matsuda J, Aburatani H, Nishino I, Ezaki O: Skeletal muscle FOXO1 (FKHR) transgenic mice have less skeletal muscle mass, down-regulated type I (slow twitch/red muscle) fiber genes, and impaired glycemic control. *J Biol Chem* 279:41114–41123, 2004
10. Nakae J, Kitamura T, Kitamura Y, Biggs WH 3rd, Arden KC, Accili D: The forkhead transcription factor Foxo1 regulates adipocyte differentiation. *Dev Cell* 4:119–129, 2003
11. Kitamura T, Nakae J, Kitamura Y, Kido Y, Biggs WH 3rd, Wright CV, White MF, Arden KC, Accili D: The forkhead transcription factor Foxo1 links insulin signaling to Pdx1 regulation of pancreatic beta cell growth. *J Clin Invest* 110:1839–1847, 2002
12. Furuyama T, Kitayama K, Yamashita H, Mori N: Forkhead transcription factor FOXO1 (FKHR)-dependent induction of PDK4 gene expression in skeletal muscle during energy deprivation. *Biochem J* 375:365–371, 2003
13. Kamei Y, Mizukami J, Miura S, Suzuki M, Takahashi N, Kawada T, Taniguchi T, Ezaki O: A forkhead transcription factor FKHR up-regulates lipoprotein lipase expression in skeletal muscle. *FEBS Lett* 536:232–236, 2003
14. Tsuchida A, Yamauchi T, Ito Y, Hada Y, Maki T, Takekawa S, Kamon J, Kobayashi M, Suzuki R, Hara K, Kubota N, Terauchi Y, Froguel P, Nakae J, Kasuga M, Accili D, Tobe K, Ueki K, Nagai R, Kadowaki T: Insulin/Foxo1 pathway regulates expression levels of adiponectin receptors and adiponectin sensitivity. *J Biol Chem* 279:30817–30822, 2004
15. Baker BF, Condon TP, Koller E, McKay RA, Siwkowski AM, Vickers TA, Monia BP: Discovery and analysis of antisense oligonucleotide activity in cell culture. *Methods* 23:191–198, 2001
16. Chou CJ, Haluzik M, Gregory C, Dietz KR, Vinson C, Gavrilova O, Reitman ML: WY14,643, a peroxisome proliferator-activated receptor alpha (PPARalpha) agonist, improves hepatic and muscle steatosis and reverses insulin resistance in lipoatrophic A-ZIP/F-1 mice. *J Biol Chem* 277:24484–24489, 2002
17. Colombo C, Haluzik M, Cutson JJ, Dietz KR, Marcus-Samuels B, Vinson C, Gavrilova O, Reitman ML: Opposite effects of background genotype on muscle and liver insulin sensitivity of lipoatrophic mice: role of triglyceride clearance. *J Biol Chem* 278:3992–3999, 2003
18. Kim JK, Fillmore JJ, Chen Y, Yu C, Moore IK, Pypaert M, Lutz EP, Kako Y, Velez-Carrasco W, Goldberg IJ, Breslow JL, Shulman GI: Tissue-specific overexpression of lipoprotein lipase causes tissue-specific insulin resistance. *Proc Natl Acad Sci U S A* 98:7522–7527, 2001
19. Samuel VT, Liu ZX, Qu X, Elder BD, Bilz S, Befroy D, Romanelli AJ, Shulman GI: Mechanism of hepatic insulin resistance in non-alcoholic fatty liver disease. *J Biol Chem* 279:32345–32353, 2004
20. Ye JM, Iglesias MA, Watson DG, Ellis B, Wood L, Jensen PB, Sorensen RV, Larsen PJ, Cooney GJ, Wassermann K, Kraegen EW: PPARalpha /gamma ragaglitazar eliminates fatty liver and enhances insulin action in fat-fed rats in the absence of hepatomegaly. *Am J Physiol Endocrinol Metab* 284: E531–E540, 2003
21. Petersen KF, Oral EA, Dufour S, Befroy D, Ariyan C, Yu C, Cline GW, DePaoli AM, Taylor SI, Gorden P, Shulman GI: Leptin reverses insulin resistance and hepatic steatosis in patients with severe lipodystrophy. *J Clin Invest* 109:1345–1350, 2002
22. Dowell P, Otto TC, Adi S, Lane MD: Convergence of peroxisome proliferator-activated receptor gamma and Foxo1 signaling pathways. *J Biol Chem* 278:45485–45491, 2003
23. Peng B, Andrews J, Nestorov I, Brennan B, Nicklin P, Rowland M: Tissue distribution and physiologically based pharmacokinetics of antisense phosphorothioate oligonucleotide ISIS 1082 in rat. *Antisense Nucleic Acid Drug Dev* 11:15–27, 2001
24. Nakae J, Biggs WH 3rd, Kitamura T, Cavenee WK, Wright CV, Arden KC, Accili D: Regulation of insulin action and pancreatic beta-cell function by mutated alleles of the gene encoding forkhead transcription factor Foxo1. *Nat Genet* 32:245–253, 2002
25. McKay RA, Miraglia LJ, Cummins LL, Owens SR, Sasmor H, Dean NM: Characterization of a potent and specific class of antisense oligonucleotide inhibitor of human protein kinase C-alpha expression. *J Biol Chem* 274:1715–1722, 1999
26. Graham MJ, Crooke ST, Monteith DK, Cooper SR, Lemonidis KM, Stecker KK, Martin MJ, Crooke RM: In vivo distribution and metabolism of a phosphorothioate oligonucleotide within rat liver after intravenous administration. *J Pharmacol Exp Ther* 286:447–458, 1998
27. Vickers TA, Koo S, Bennett CF, Crooke ST, Dean NM, Baker BF: Efficient reduction of target RNAs by small interfering RNA and RNase H-dependent antisense agents: a comparative analysis. *J Biol Chem* 278:7108–7118, 2003
28. Youn JH, Buchanan TA: Fasting does not impair insulin-stimulated glucose uptake but alters intracellular glucose metabolism in conscious rats. *Diabetes* 42:757–763, 1993
29. Bligh EG, Dyer WJ: A rapid method of total lipid extraction and purification. *Can J Med Sci* 37:911–917, 1959
30. Neschen S, Moore I, Regittnig W, Yu CL, Wang Y, Pypaert M, Petersen KF, Shulman GI: Contrasting effects of fish oil and safflower oil on hepatic peroxisomal and tissue lipid content. *Am J Physiol Endocrinol Metab* 282:E395–E401, 2002
31. Yu C, Chen Y, Cline GW, Zhang D, Zong H, Wang Y, Bergeron R, Kim JK, Cushman SW, Cooney GJ, Atcheson B, White MF, Kraegen EW, Shulman GI: Mechanism by which fatty acids inhibit insulin activation of insulin receptor substrate-1 (IRS-1)-associated phosphatidylinositol 3-kinase activity in muscle. *J Biol Chem* 277:50230–50236, 2002